SAND2017-8242J

AN APPROACH TO QUAD MESHING BASED ON HARMONIC CROSS-VALUED MAPS AND THE GINZBURG-LANDAU THEORY*

RYAN VIERTEL† AND BRAXTON OSTING†

Abstract. A generalization of vector fields, referred to as N-direction fields or cross fields when $N = 4$, has been recently introduced and studied for geometry processing, with applications in quadrilateral (quad) meshing, texture mapping, and parameterization. We make the observation that cross field design for two-dimensional quad meshing is related to the well-known Ginzburg-Landau problem from mathematical physics. This identification yields a variety of theoretical tools for efficiently computing boundary-aligned quad meshes, with provable guarantees on the resulting mesh, for example, the number of mesh defects and bounds on the defect locations. The procedure for generating the quad mesh is to (i) find a complex-valued "representation" field that minimizes the Dirichlet energy subject to a boundary constraint, (ii) convert the representation field into a boundary-aligned, smooth cross field, (iii) use separatrices of the cross field to partition the domain into four sided regions, and (iv) mesh each of these four-sided regions using standard techniques. Under certain assumptions on the geometry of the domain, we prove that this procedure can be used to produce a cross field whose separatrices partition the domain into four sided regions. To solve the energy minimization problem for the representation field, we use an extension of the Merriman-Bence-Osher (MBO) threshold dynamics method, originally conceived as an algorithm to simulate motion by mean curvature, to minimize the Ginzburg-Landau energy for the optimal representation field. Finally, we demonstrate the method on a variety of test domains.

Key words. Cross Fields, N-direction Fields, Quad Meshing, Ginzburg-Landau Theory, Computational Geometry, Geometry Processing

AMS subject classifications. 35Q56, 65N50, 68U05

1. Introduction.

A generalization of vector fields, referred to as *N-direction fields* allow for N directions to be encoded at each point of a domain. When $N = 4$ the term *cross field* is often used. Such fields are better suited to encode multidirectional information than simply using N overlaid vector fields because they can encode singularities of "fractional index" in the neighborhood of which an N-direction field turns $2\pi/N$ radians (see Figure 1). N-direction fields have found recent applications in quad re-meshing for computer graphics and finite element simulations [8, 15, 17, 21, 32], parameterization [29, 33], non-photorealistic rendering [13], and texture mapping [19]. This paper will focus mainly on cross fields and their application in quad meshing for finite element methods.

Various methods have been proposed to generate a quad mesh on a domain using a cross field (see subsection 2.0.2). One basic procedure, identical to the approach taken in [21], is illustrated in Figure 2. In the top left panel we have a domain, U, with outward normal boundary vectors indicated. In the top right a complex-valued "representation" field that minimizes the Dirichlet energy subject to a boundary condition and a unit norm constraint is found. In the bottom left the representation field is converted into a boundary-aligned, smooth cross field. Seperatrices of the cross field are computed which partition the domain into four sided regions. Finally, the

*August 1, 2017

Funding: R. Viertel is supported by Sandia National Laboratories. Sandia National Laboratories is a multi-mission laboratory managed and operated by National Technology & Engineering Solutions of Sandia, LLC., a wholly owned subsidiary of Honeywell International, Inc., for the U.S. Department of Energy's National Nuclear Security Administration under contract DE-NA0003525. B. Osting is partially supported by NSF DMS 16-19755.

†Department of Mathematics, University of Utah, Salt Lake City, UT (viertel@math.utah.edu, osting@math.utah.edu).

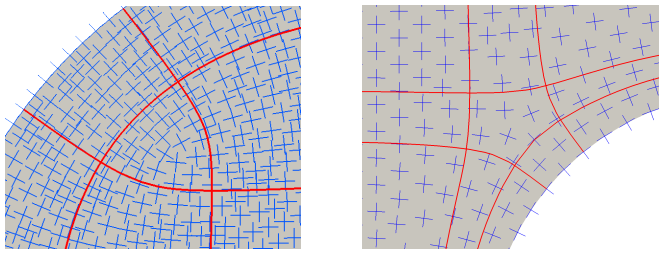

FIG. 1. **Singularities of index $+1/4$ and $-1/4$. (left)** *A singularity with index $+1/4$ is contained in the region enclosed by the three red lines, which are streamlines of the cross field. Since the index is $+1/4$, the cross field makes a quarter turn counterclockwise when circulating around this singularity.* **(right)** *Similarly, a singularity with index -1/4 is enclosed by the 5 red lines. The cross field makes a quarter turn clockwise when circulating around this singularity.*

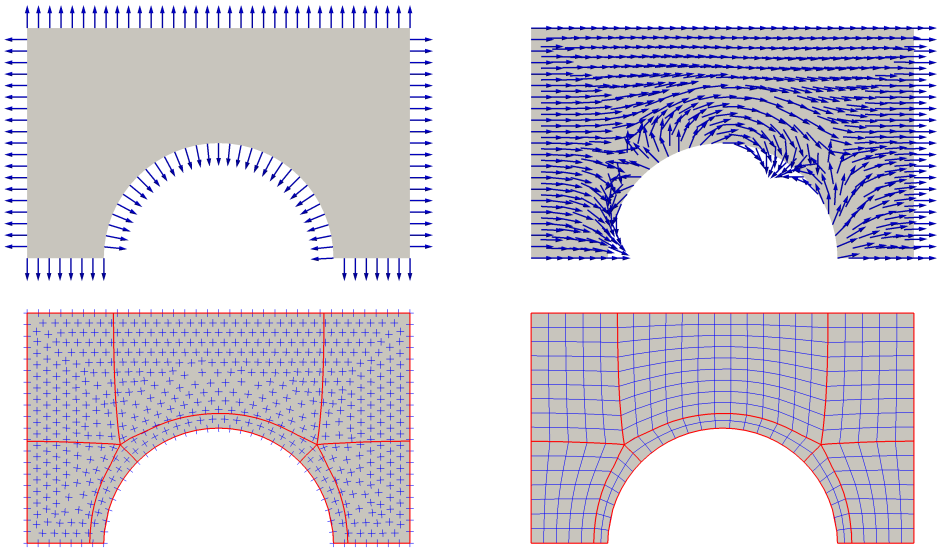

FIG. 2. **Overview of the cross field based meshing methods. (top left)** *The domain is shown with outward pointing normals.* **(top right)** *A 4-aligned boundary condition is assigned (see Definition 3.12) and a representation vector field is found by approximately minimizing the Ginzburg-Landau energy.* **(bottom left)** *The representation field is mapped to a smooth cross field and separatrices of the cross field are traced to partition the domain into a quad layout.* **(bottom right)** *A regular mesh is mapped into each region.*

bottom right panel shows a regular mesh mapped into each of the four-sided regions.

1.1. Contributions. In this paper, we consider the problem of cross field generation and cross field guided quad meshing. We make the observation that cross field design for quad meshing is related to the Ginzburg-Landau theory from mathematical physics. In particular, many of the computational methods currently used for cross field design are minimizing an energy that is, or is very similar to, a discrete Ginzburg-Landau energy; see, for example, [3, 8, 15, 16, 21, 31, 37, 36].

We make this correspondence precise and use results from the Ginzburg-Landau theory to prove, in Theorems 5.6 and 5.9, that the separatrices of a harmonic cross field with indices $\leq 1/4$ partition a domain into four-sided regions, possibly with a T-

junction if a limit cycle is present. The corners of these four-sided regions are located at the singularities of the harmonic cross field. The proof of this result depends on an asymptotic analysis of the cross field near singularities, which uses results from the Ginzburg-Landau theory; see subsection 5.1. Because we consider domains with corners, we also make precise a notion of boundary singularities (see Definition 5.3) and study their properties. We show, in Lemma 5.5, the structure of a boundary singularity with these definitions is consistent with the structure of a cross field near an (interior) singularity. In addition, topological results from the Ginzburg-Landau theory as well as the renormalized energy that describes the positions of singularities gives provable guarantees for this partition with four-sided regions. Based on these results, we develop an algorithm (Algorithm 1) that uses a harmonic cross field to partition a domain into four-sided regions, possibly with T-junctions.

To find a harmonic cross field, we approximately minimize the Ginzburg-Landau energy and find a suitable representation field by using a generalization of the MBO algorithm (Algorithm 2) [27]. This results in a harmonic cross field with isolated singularities of degree $\pm 1/4$. This can then be used as input for Algorithm 1 to find a partition with four-sided regions. The partition can then be used to generate a high-quality quad mesh on the domain with standard techniques.

Finally, we use our cross field design algorithm and partitioning theorem to design quad meshes for several example geometries; see Figure 11. Throughout, we also include figures, generated using the algorithms described in this paper, to illustrate the main ideas.

Outline. In section 2, we review previous work. In section 3 we recall some background material and establish nomenclature for the paper. In section 4, we describe a connection between quad meshing and the Ginzburg-Landau theory. In section 5, we use the Ginzburg-Landau theory to prove results about quad meshes. In section 6 we discuss computational methods. We conclude in section 7 with a discussion.

2. Previous work.

The problem of building a quad mesh via a cross field is two-fold, and consequently most works in the field fall into two categories: papers that are concerned with cross field design [12, 18, 37] and papers that are concerned with meshing [6, 17, 29, 30]. There are some which cover both topics [8, 15, 20]. Here we present a selection of works that have contributed to the understanding of fundamental issues in the cross field design and meshing problems. For brevity, we only review the work that is most relevant to this paper, however excellent literature reviews are available on cross field and directional field design [47] and recent approaches to quad meshing [7].

2.0.1. Cross field design.

Each cross field design algorithm must choose a way to represent a cross. In particular, it is necessary that the representative object exhibit $\pi/2$-rotational symmetry. A pair of orthogonal vectors is inadequate unless an identification is made between the two vectors. In [22], an integer variable called a *period jump* was introduced between any two crosses on a discrete triangle mesh that explicitly encoded the ambiguous matching between vectors. In [31], a representation referred to as the N-RoSy representation was introduced, based on the periodic representation in [33]. In the N-RoSy representation, a cross in 2D is represented by a vector on S^1, where the angle the vector makes with a reference axis is four times the angle that the nearest component of the cross makes with that reference axis; see Figure 3. The advantage of such a representation is that the matching between

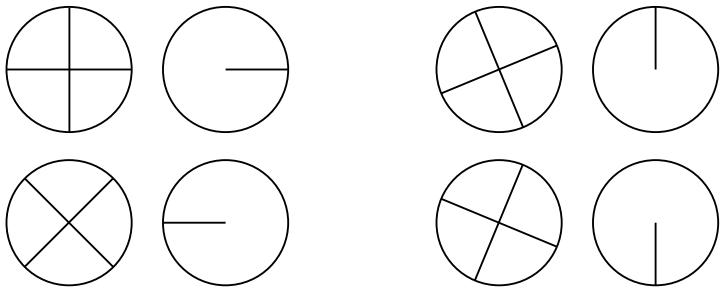

FIG. 3. **The representation map for cross fields.** *The left figure for each pair represents an element of C_4 (see Definition 3.8), visualized by a line from zero to the representative numbers on the unit circle. The right figure shows the representation as a line from zero to $[c]^4$. This representation is equivalent to the N-RoSy representation, only expressed in complex numbers.*

adjacent crosses is implicit, and there is no need to introduce an integer variable to control the matchings. The N-RoSy representation is also defined in the continuum, not just as a discrete construction. Subsequent work has used some variation of the N-RoSy representation [3, 16, 18, 21] or has opted to use period jumps to explicitly define the matchings [8, 15, 37].

Most cross field design papers have approached the problem of generating a smooth field by an energy minimization technique. Because of the close ties in this field of research with software applications, these energies are often only defined in the discrete setting. The typical measure of field smoothness is a discrete version of the Dirichlet energy: the sum of squared differences of some quantity representing the cross orientation at each point. For formulations using the N-RoSy representation [16, 21, 31], this is the discrete Dirichlet energy of the representation vector. Since only unit vectors are representative of crosses, a point-wise unit norm constraint is applied to each vector, limiting the search space of the minimization problem to allow only unit vector fields. As we will establish in section 4, the continuous analogue of this problem is exactly the problem considered in the Ginzburg-Landau theory.

In approaches which use period jumps [8, 22, 37], the energy consists of the squared differences of angles representing the orientation of each cross. Since there is ambiguity in choosing how the vectors match up in two adjacent crosses, an integer variable called a *period jump* is required to encode this information. Its appearance in the energy functional makes the minimization problem a mixed integer problem. Though this energy has not been extended to a continuous setting, the quantity being minimized is a discrete Dirichlet energy of a scalar function representing the angle that a cross makes with a reference direction at each point in the domain. In the case of a domain where singularities are not topologically necessary, there is no need for period jump variables in the definition of the energy. Setting each period jump variable to zero, the energy becomes exactly a discretization of the Dirichlet energy of the angle. The results of section 4 show that minimizing the Dirichlet energy of the cross angle is equivalent to minimizing the Ginzburg-Landau energy; see Theorem 4.5 and the preceding example.

Beaufort et al. [3] have also recently recognized the connection between the Ginzburg-Landau model and cross field generation. They use the N-RoSy representation and minimize the Ginzburg-Landau energy using a Newton method. Many of these ideas have appeared in earlier work on cross field design [8, 15, 21, 22, 31, 37],

e.g., the discrete energies formulated approximately minimize a Ginzburg-Landau type energy, though the connection to Ginzburg-Landau theory is not explicitly made.

There are two cross field design algorithms that we are aware of that are fundamentally different than the above algorithms. The first is by Crane et al. [11]. This algorithm builds N-direction fields on a surface with a known set of singularities by solving for *trivial connections* on the surface, and then simply parallel transporting a given reference N-direction across the entire surface. On a flat surface this reduces to simply a constant field. This is fundamentally different from our problem because we wish to design a harmonic field on the domain that meets a specified boundary condition. The second paper is by Knöppel et al. [18]. In this paper, the energy of a cross field is defined as the minimum Dirichlet energy of any scaling of the field. This allows the representation vectors near singularities to approach zero, and removes the necessity of applying a point-wise unit vector constraint. Unlike Ginzburg-Landau type approaches, with this definition the singularities carry finite energy (see section 4). Further, the energy is convex, guaranteeing that a globally optimal solution can be found by solving a sparse linear system of size that is linear in the number of mesh elements.

2.0.2. Cross field guided meshing. Most cross field driven quad meshing techniques fall into two categories: streamline tracing techniques and parameterization techniques. While parameterization techniques have found success in some commercial applications and received more attention in early research [8, 6, 17], we choose to focus on streamline tracing methods because of their direct connection with the topology of the cross field. We refer the reader interested in parameterization based meshing techniques to [7].

Streamline tracing methods decompose the geometry into four-sided regions by tracing separatrices of the cross field. Alliez et al. [1] produced quad dominant meshes by tracing streamlines in principle curvature directions and filling in flat areas with triangle elements. Kowalski et al. [21] implemented a streamline tracing algorithm in flat 2D by tracing streamlines starting at singularities and continuing until the streamline reaches either the boundary of the domain or another singularity. This approach works well on most domains but can fail on geometries with limit cycles. Naive streamline tracing algorithms have the disadvantage that parallel streamlines can intersect due to numerical inaccuracies. Ray and Sokolov [34] and Myles and Zorin [29] independently developed robust streamline tracing methods such that prevent such errors. Further, Myles and Zorin [29] developed a robust algorithm to partition a 2-manifold into four-sided regions and demonstrated its robustness on a database of 100 objects.

3. Background, assumptions, and basic definitions. Throughout this paper, we will make the following assumptions about the geometric domain to be meshed.

ASSUMPTION 3.1. *The domain $D \subset \mathbb{R}^2$ is a bounded, simply connected planar domain with a piecewise smooth boundary.*

The theorems for the Ginzburg-Landau Theory in section 4 require a smooth boundary, however many domains of interest for the meshing problem have corners. For theoretical results sections 4 and 5, we smooth each corner of the domain with a Bézier curve with three control points, one on the corner, and two on the boundary at a distance $\varepsilon \ll 1$ from the corner. The boundary condition along the smooth curve is then assigned by linearly interpolating the cross with the angle of inclination above

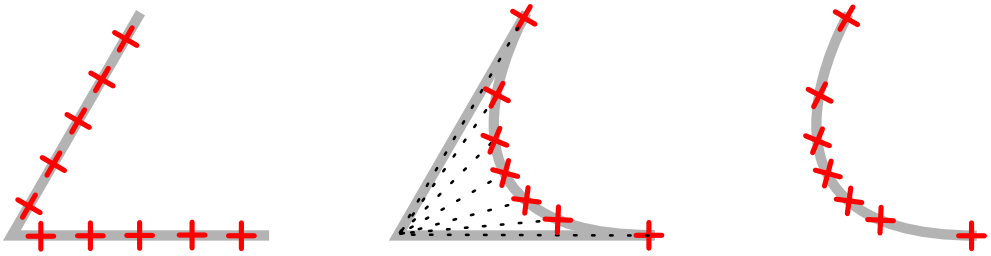

FIG. 4. **(left)** *The cross field along a sharp corner with index* 1/4*. The cross turns* 90° *counterclockwise with respect to the direction of the curve, all at a single point.* **(center)** *Transformation between a sharp corner and a smooth curve, the crosses turn smoothly with the angle of inclination.* **(right)** *The cross field along a smooth curve turning* 90° *counterclockwise with respect to the direction of the curve.*

the corner, and then propagated back onto the domain constant along each ray; see Figure 4. In practice there is no need to apply this smoothing operation; as described in section 6, we approximate the domain with linear finite elements which have a similar effect. Multiply connected domains can be handled using the framework within this paper by cutting the domain, or handled directly by applying the results in [38]. We expect that many of the results in this paper can be generalized to *surfaces* with piecewise smooth boundary.

3.1. Quad meshing.

DEFINITION 3.2. *A 2D* polygonal mesh *is a finite collection of* nodes*,* edges*, and* faces*. Each node is associated with and can be viewed as a point in* $\mathbb{R}^2$*. An* edge *is a straight line between two nodes and is said to be* bounded *by those nodes. A* face *is a surface bounded by a minimal cycle of edges; minimal meaning that removing any edge would break the cycle, and that no edge is contained in the interior of the cycle.*

DEFINITION 3.3. *A* quad mesh *is a polygonal mesh where each face is bounded by four edges. We will sometimes say* all-quad mesh *for emphasis. A* quad layout *is similar to a quad mesh, but in place of straight edges piecewise smooth curves are allowed, and further we allow for the degenerate case where a face of a quad layout is only bounded by two curves i.e., an annulus.*

DEFINITION 3.4. *A* T-junction *is a mesh feature where an internal edge contains an extra node called a* free node*, which bounds only one edge.*

The mesh in Figure 9(right) contains a T-junction.

DEFINITION 3.5. *The* valence *of a node is the number of edges it bounds. An internal node of a quad mesh is* irregular *if its valence is not four. A boundary node of a quad mesh is irregular if its valence is not three.*

DEFINITION 3.6. *A* string *of edges of a quad mesh is the set of edges formed by starting with a given edge, and recursively adding to the set all edges on a regular node that are opposite to an edge in the current set. By construction, each* string *terminates at an irregular node, or at the boundary.*

DEFINITION 3.7. *The* skeleton *of a quad mesh is the set of all strings beginning at irregular nodes of the mesh along with all boundary edges.*

The skeleton of the quad meshes in Figure 2(bottom right), Figure 7(bottom right), and Figure 11(right) are colored in red.

3.2. Cross fields.

DEFINITION 3.8. *Let* $\mathbb{T} = \{z \in \mathbb{C} \colon |z| = 1\}$ *be the circle group with group operation given by complex multiplication and let* $\rho(N)$ *be the set of the* N*th roots of unity. An* N-direction *is an element of* $C_N = \mathbb{T}/\rho(N)$*. A 4-direction is also called a* cross.

DEFINITION 3.9. *There is a canonical group isomorphism* $R \colon C_N \to \mathbb{T}$ *called the* representation map *given by*

$$R([c]) = c^N,$$

where c *is any representative member of the equivalence class* $[c] \in C_N$*. The* inverse representation map $R^{-1} \colon \mathbb{T} \to C_N$ *is given by*

$$R^{-1}(u) = \left[\sqrt[N]{u} \right],$$

i.e. by choosing the equivalence class of the N*th roots of* u*.*

In the literature, an N-direction, $[c] \in C_N$, is often visualized as an unordered set $\{v_0, v_1, \ldots, v_{N-1}\}$ of N unit vectors, each one pointing from the origin towards the N representative elements of the class $[c]$. Clearly, an N-direction has a rotational symmetry of $2\pi/N$. An example of a cross field is illustrated in Figure 2 (bottom left).

DEFINITION 3.10. *An* N-direction field *on* D *is a map* $f \colon D \to C_N \cup \{0\}$ *where only finitely many points are mapped to zero. The map* $R \circ f \colon D \to \mathbb{T}$ *obtained by composing the representation map with an* N*-direction field,* f *is called the* representation field for f*.*

DEFINITION 3.11. *Let* $N(f)$ *be the zero set of an* N*-direction field,* f*. Then* f *is* smooth *if* $R \circ f \colon D \setminus N(f) \to \mathbb{T}$ *is a smooth map. Similarly,* f *is* harmonic *if* $R \circ f$ *is harmonic on* $D \setminus N(f)$*, i.e. satisfies* $\Delta(R \circ f) = 0$*.*

DEFINITION 3.12. *Let* $\nu = (\nu^1, \nu^2)$ *be the outward pointing unit normal vector on* ∂D*, and let* $c_\nu = (\nu^1 + i\nu^2)$*. If a map* $g \colon D \to \mathbb{T}$ *is such that* $g = c_\nu^N$ *for every smooth point* $p \in \partial D$*, then* g *is said to be* N-aligned *to the boundary of* D*. If* $f \colon D \to C_N$ *is an* N*-direction field on* D *such that* $R \circ f|_{\partial D} = c_\nu^N$*, then* f *is said to be* boundary-aligned *to* D*.*

DEFINITION 3.13. *Let* $\gamma \colon [0, 1] \to D$ *be a simple closed curve circulating a single zero of the map* f *at an interior point* p *of* D*. Then the value*

$$\mathrm{I}(p) := \frac{\arg R(f(\gamma(1))) - \arg R(f(\gamma(0)))}{2\pi N}$$

is the index *of* p*. The zero* p *is called a* singularity *of the* N*-direction field if its index is not zero. The index of a singularity of an* N*-direction field is* $1/N$ *times the index of the corresponding singularity of the representation field.*

Note: The argument in Definition 3.13 can be chosen arbitrarily at $\gamma(0)$ but after varies smoothly along γ.

3.2.1. Streamlines.

A characteristic trait of a smooth vector field is that away from zeros it locally foliates the space, meaning that streamlines of the vector field partition the space into disjoint curves [24]. Streamlines can be similarly defined for an N-direction field except that these streamlines can intersect themselves and each other at angles of $2\pi/N$, as we make precise below.

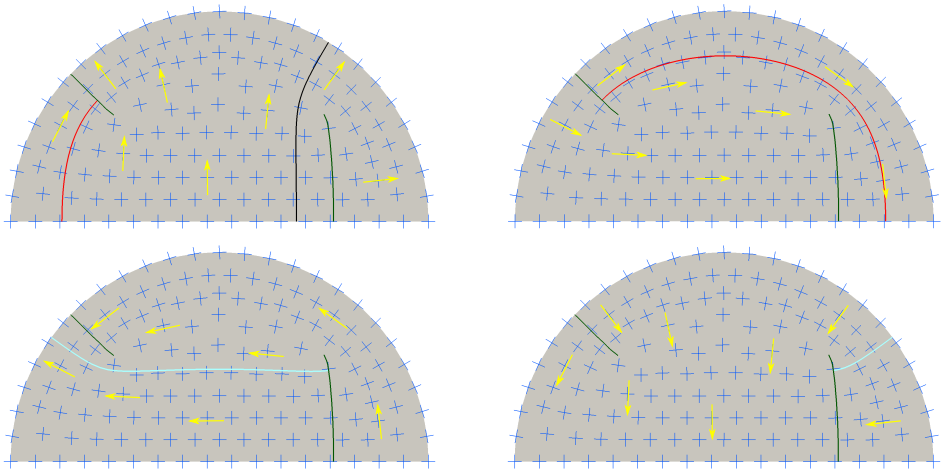

FIG. 5. *The covering vector field and the four sheets of the Riemann surface for the half disk. The red and cyan streamlines both cross a green branch cut, causing the streamline to change sheets. The red, black, and cyan streamlines of the covering vector field project onto the base domain as streamlines of the cross field.*

For the representation field $R \circ f \colon D \to \mathbb{T}$ of the N-direction field f on D, the map $\Lambda_N \colon D \to \mathbb{T}$ defined by $\Lambda_N = \sqrt[N]{R(f)}$ is a multi-valued map on D. We can make a branch cut from each of the singularities of $R(f)$ to the boundary, and define a Riemann surface, $\mathcal{R}$ for this choice of branch cuts.

DEFINITION 3.14. *The* covering vector field *on D for the given N-direction field f and choice of branch cuts of Λ_N is the smooth vector field $\widehat{\Lambda}_N \colon \mathcal{R} \to \mathbb{T}$ defined by assigning the vector pointing from the origin to $\Lambda_N(p)$ at each point p of $\mathcal{R}$.*

The initial observation that a cross field has a corresponding smooth vector field on a 4-covering of the domain of definition is accredited to Kälberer et al. [17].

DEFINITION 3.15. *Let $\gamma_N \colon [a,b] \to \mathcal{R}$ be a streamline of $\widehat{\Lambda}_N$, satisfying $\frac{d\gamma_N}{dt} = \widehat{\Lambda}_N(\gamma(t))$ for $t \in [a,b]$. Then the function $\gamma \colon [a,b] \to D$ given by*

$$\gamma = \pi \circ \gamma_N$$

is a streamline *of the N-direction field f. A* separatrix *of an N-direction field is a streamline that begins or ends at a singularity.*

Figure 5 shows an illustration of the covering field for a cross field on a half disk. The two green lines are branch cuts that join a singularity to a point on the boundary. Several example streamlines are drawn. For example, the red streamline in the top left panel is continued in the top right panel.

No two streamlines of $\widehat{\Lambda}_N$ can intersect each other on $\mathcal{R}$, thus, if streamlines of the N-direction field were to intersect at a point $p \in D$, they could only do so if $\pi^{-1}(\gamma)|_p$ is on two different covers of $\mathcal{R}$. Thus we conclude that streamlines of an N-direction field can only intersect themselves and each other at integer multiples of the angle $2\pi/N$; see, *e.g.*, Figure 11 (bottom center).

4. Correspondence between cross field design and the Ginzburg-Landau theory. As mentioned in section 2, the cross field design problem is often formulated

as finding harmonic cross fields, or equivalently as an energy minimization problem with a feasibility constraint. Approaches using the N-RoSy representation for a cross field, f, use the Dirichlet energy for the representation map, given by

$$E[R(f)], \qquad \text{where} \quad E[u] := \frac{1}{2}\int_D |\nabla u|^2 dA. \tag{1}$$

The problem then is to find the minimizer among all complex fields that can feasibly represent a cross field:

$$\inf_{u \in H^1_g(D;\mathbb{T})} E(u) \tag{2}$$

where

$$H^1_g(D;\mathbb{T}) := \{u \in H^1(D;\mathbb{C}) \colon \ u(x) = g(x)\ \forall x \in \partial D \ \text{ and } \ |u(x)| = 1 \text{ a.e. } x \in D\}.$$

Here, g is an N-aligned boundary condition (see Definition 3.12), and the feasibility constraint $|u(x)| = 1$ keeps the solution on the unit circle so that a cross can be defined at a point x by $R^{-1}(u(x))$.

The admissible set in (2), $H^1_g(D,\mathbb{T})$, is empty for any topology that requires a singularity [4]. Indeed, the Dirichlet energy (1) is infinite for functions with singularities [4, 18]. This is problematic because, by the Poincaré-Hopf theorem, a boundary-aligned field will require singularities for many geometries of interest. Problem (2) can be relaxed by enlarging the admissible set to $H^1_g(D,\mathbb{C})$, so that the solution can approach zero in the neighborhood of a singularity. A penalty term can then be added to the Dirichlet energy given the minimization problem

$$\inf_{u \in H^1_g(D,\mathbb{C})} E_\varepsilon(u) \qquad \text{where} \quad E_\varepsilon(u) = \frac{1}{2}\int_D |\nabla u|^2 dA + \frac{1}{4\varepsilon^2}\int_D (u^2-1)^2 dA. \tag{3}$$

This is the approach taken in the study of the Ginzburg-Landau theory. In their foundational work on Ginzburg-Landau vortices, Betheul et al. show that there is a well-defined sense in which generalized solutions to (2) can be understood as solutions to (3) in the limit $\varepsilon \to 0$. The following results of the Ginzburg-Landau theory can be applied to N-direction field design

Definition 4.1. *The* Brouwer degree *of a map $g\colon \partial D \to \mathbb{T}$, written $d = deg(g, \partial D)$, is the number of times that $g(s)$ wraps around $\mathbb{T}$ as s traverses ∂D.*

Theorem 4.2 ([4, Theorem 0.1]). *Let $D \subset \mathbb{R}^2$ be a bounded, simply connected domain with smooth boundary* [1] *and let $g\colon \partial D \to \mathbb{T}$ be a smooth function. Let $d = \deg(g, \partial D)$ be the Brouwer degree of g on ∂D. Denote by u_ε a solution of (3) for $\varepsilon > 0$. Given a sequence $\varepsilon_n \to 0$ there exists a subsequence ε_{n_i} and exactly d points $a_1, a_2, ..., a_d$ in $D \subset \mathbb{C}$ and a smooth harmonic map $u_\star\colon D \setminus \{a_1, ..., a_d\} \to \mathbb{T}$ with $u_\star = g$ on ∂D such that*

$$u_{\varepsilon_{n_i}} \to u_\star \qquad \text{in} \ \ C^k_{loc}(D \setminus \bigcup_i (a_i)) \ \ \forall k \ \ \text{and in} \ \ C^{1,\alpha}(\bar{D} \setminus \bigcup_i (a_i)) \ \ \forall \alpha < 1.$$

In addition, if $d \neq 0$, each singularity of $u_\star$ has index $\operatorname{sgn}(d)$ and, more precisely, there are complex constants, α_i, with $|\alpha_i| = 1$ such that

$$\left| u_\star(z) - \alpha_i \frac{z - a_i}{|z - a_i|} \right| \leq C|z - a_i|^2 \qquad as \qquad z \to a_i, \quad \forall i.$$

[1] Theorems 4.2 and 4.3 are stated in [4] for star shaped domains, but this assumption was relaxed to simply connected domains in [44].

In other words, Theorem 4.2 guarantees a sequence of minimizers of the relaxed problem (3) that converges to a function, $u_\star$, that is harmonic on $D \setminus \{a_1, ..., a_d\}$. Thus we can think of $u_\star$ as a generalized solution of the minimization problem (2).

THEOREM 4.3 ([4, Corollary I.1]). *Let $D \subset \mathbb{R}^2$ and $g\colon \partial D \to \mathbb{T}$ be as in Theorem 4.2 with $d = \deg(g, \partial D)$. Given any configuration $a = \{a_1, \dots, a_n\}$ of distinct points $a_j \in D$ with indices $I = \{d_1, \dots, d_n\}$ satisfying $d = \sum_{i=1}^n d_i$, there is a unique function u_0 satisfying*

(i) u_0 is a smooth harmonic map from $D \setminus \cup_i a_i$ to $\mathbb{T}$,
(ii) $u_0 = g$ on ∂D, and
(iii) for some complex numbers α_j with $|\alpha_j| = 1$,

$$\left| u_0(z) - \alpha_j \frac{(z-a_j)^{d_j}}{|z-a_j|^{d_j}} \right| \leq C|z-a_j| \quad \text{as} \quad z \to a_j, \quad \forall i. \tag{4}$$

Furthermore, u_0 is given by

$$u_0 = e^{i\varphi(z)} \, \frac{(z-a_1)^{d_1}}{|z-a_1|^{d_1}} \, \frac{(z-a_2)^{d_2}}{|z-a_2|^{d_2}} \, \cdots \, \frac{(z-a_n)^{d_n}}{|z-a_n|^{d_n}},$$

where φ is the solution of the Dirichlet problem

$$\Delta\varphi = 0 \qquad \text{in } D \tag{5a}$$
$$\varphi = \varphi_0 \qquad \text{on } \partial D, \tag{5b}$$

and φ_0 is defined on ∂D by

$$e^{i\varphi_0(z)} = g(z) \, \frac{|z-a_1|^{d_1}}{(z-a_1)^{d_1}} \, \frac{|z-a_2|^{d_2}}{(z-a_2)^{d_2}} \, \cdots \, \frac{|z-a_n|^{d_n}}{(z-a_n)^{d_n}}. \tag{6}$$

DEFINITION 4.4. *The smooth harmonic map $u_0\colon D \setminus \cup_i a_i \to \mathbb{T}$ in Theorem 4.3 is called the* canonical harmonic map *associated with the boundary condition g, and singularity configuration with locations $a = \{a_1, \dots, a_n\}$ and indices $I = \{d_1, \dots, d_n\}$. The N-direction field associated with the canonical harmonic map, defined by $R^{-1}(u_0)$ is called the* canonical harmonic N-direction field *associated with (g, a, I).*

For a given boundary condition and configuration of singularities, the canonical harmonic map has the smallest Dirichlet energy (1) (in a generalized sense). Figure 6 displays streamlines of cross fields having the same geometry and boundary condition but different singularity configurations. Each of these cross fields was generated using the explicit formulation from Theorem 4.3.

Example: domain with zero Brouwer degree. The case of a domain with zero Brouwer degree helps to understand Theorem 4.3. If the Brouwer degree, d, is zero, then no singularities are required, and equation (6) simplifies to $e^{i\varphi_0(z)} = g(z)$ for $z \in \partial D$, *i.e.*, $\varphi_0(z)$ is simply the smoothly varying angle that $g(z)$ makes with the x-axis. Since d is zero, $\varphi_0(z)$ will return to its original value after circulating the geometry. Thus the cross field can be unambiguously encoded by its angle of inclination. The angle defined on the boundary is smoothly propagated into the domain by solving (5), and transformed into elements of $\mathbb{T}$ simply by exponentiating the angle. Another result by Bethuel *et. al.* [4] shows that (5) is equivalent to the Ginzburg-Landau problem on domains with Brouwer degree zero.

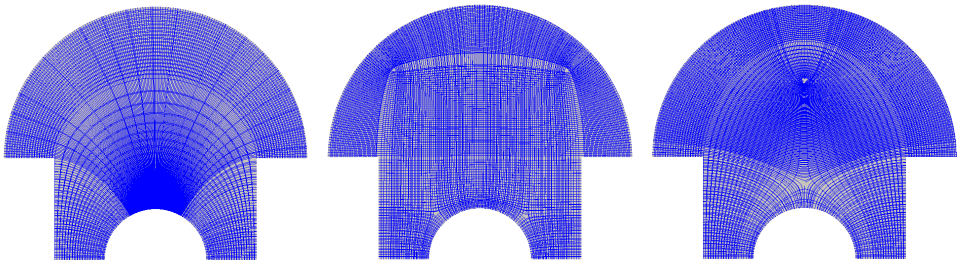

FIG. 6. *A plot of the streamlines for multiple smooth cross fields on a "mushroom" domain, each with different singularity configuration. The Brouwer degree of this domain is zero.* **(left)** *This is the boundary-aligned canonical harmonic cross field with no singularities, which by Theorem 4.5 is the global minimizer of the Ginzburg-Landau energy.* **(center)** *This cross field has four singularities. The top two have degree $+1/4$ and the bottom two have degree $-1/4$.* **(right)** *This cross field has two singularities. The top one has degree $+1/2$ and the bottom one has degree $-1/2$.*

THEOREM 4.5 ([4, Theorem 0.3]). *Let d be the Brouwer degree for domain D, $\{a_1, \dots, a_d\}$ be the singularity positions, and $u_\star$ be the minimizer of the Ginzburg-Landau energy with boundary condition g as in Theorem 4.2. Then $u_\star$ is the canonical harmonic map for the boundary condition g and singularity configuration $\{a_1, \dots, a_d\}$ with indices* $\operatorname{sgn}(d)$.

On a domain with Brouwer degree zero, the minimizer of the angle Dirichlet energy is the canonical harmonic map for the empty singularity configuration, which by Theorem 4.5 is exactly the minimizer of the Ginzburg-Landau problem.

4.1. Renormalized energy, singularity location, and index. Theorem 4.2 tells us that the *global minimizer* of (2) will have isolated singularities occurring on the interior of D each with index $\operatorname{sgn}(d)$. For practical applications such as meshing, we cannot rely on finding a global minimizer as the problem is non-convex. The Ginzburg-Landau theory offers some results that can be extended to local minimizers as well. In particular, it tells us that the singularities of a local minimizer will not occur on the boundary, be placed too close together, or have index with magnitude > 1. A similar discussion appears in [3].

DEFINITION 4.6. *The* renormalized energy, *W, of a cross field f is defined as*

$$W = -\pi \sum_{i \neq j} d_i d_j \log |a_i - a_j| + \frac{1}{2} \int_{\partial D} \Phi(g \times g_\tau) - \pi \sum_{i=1}^{n} d_i R(a_i),$$

where if ν is the outward pointing unit normal on ∂D, τ is the unit tangent vector to ∂D such that (ν, τ) is direct, g_τ is the directional derivative of g in the direction τ, $R(x) = \Phi(x) - \sum_{j=1}^{n} d_j \log |x - a_j|$, and Φ is the solution of the linear Neumann problem

$$\begin{aligned} \Delta \Phi &= \sum_{i=1}^{n} 2\pi d_i \delta_{a_i} && \text{in } D \\ \frac{\partial \Phi}{\partial \nu} &= g \times g_\tau && \text{on } \partial D. \end{aligned}$$

THEOREM 4.7 ([4, Theorem I.8]). *Let u_0 be the canonical harmonic map associ-*

ated to (g, a, I)*, then as* $\rho \to 0$

$$\frac{1}{2}\int_{\Omega_\rho} |\nabla u_0|^2 \quad \to \quad \pi\left(\sum_{i=1}^{n} d_i^2\right)\log 1/\rho + W + O(\rho^2), \tag{7}$$

where $\Omega_\rho = D \setminus \bigcup_{i=1}^{n} \overline{B(a_i, \rho)}$.

The first term on the right hand side of (7) tells us that a configuration where any singularity has degree other than ± 1 can not be a local minimizer. Further, since the second term of W is bounded independent of the singularity configuration, the first term of W causes $W \to \infty$ as singularities with index of the same sign approach each other, and $R \to \infty$ as singularities approach the boundary. Thus, even for a local minimizer we can expect that the representation field will have isolated singularities of index ± 1. For further discussion see the proof of [4, Theorem I.10].

5. Cross field topology and quad mesh structure. At the heart of cross field based quad meshing methods is the notion that there is a connection between the topology of a cross field and the structure of a quad mesh. Streamline tracing methods use the cross field topology directly; by tracing separatrices of the field, they decompose the geometry into four-sided regions [21, 29]. Parameterization based methods use this connection implicitly by building a parameterization that is as aligned as possible to the cross field in a least squares sense [8, 17].

In this section, we make rigorous the connection between the topology of a harmonic cross field and the structure that can be extracted from it for use in building a quad mesh on a domain. Central to this idea is the relation between the index of a cross field singularity, and the valence of a node in a mesh. Subsections 5.1 and 5.2 contains three lemmas which make this relationship explicit. We begin with any boundary-aligned canonical harmonic cross field, not necessarily a minimizer of the Ginzburg-Landau energy. In Lemmas 5.1 and 5.4 we show that there is a relationship between the singularity index and the number of separatrices meeting at that singularity. Kowalski et al. [21] reached a similar result for discrete fields, assuming a linear interpolation across mesh elements. Beaufort et al. [3] also reach similar conclusions for cross fields that are *a priori* aligned to a quad mesh. Further, in Lemma 5.5 we show that the local topology of the cross field in each sector between separatrices is identical to that of a constant field on a 90° corner. The results of these lemmas are illustrated in Figure 7. For the sake of generality, the results in the following section are stated in terms of N-direction fields.

5.1. Behavior of N-direction fields near (interior) singularities. Our first result is that singularities locally partition an N-direction field into evenly angled sectors. The number of sectors depends only on the index of the singularity.

LEMMA 5.1. *Let* f *be a boundary-aligned canonical harmonic* N*-direction field on* D*. Let* a *be an interior singularity of* f *of index* d/N *with* $d < N$*. There are exactly* $N - d$ *separatrices meeting at* a*. These separatrices partition a neighborhood of* a *into* $N - d$ *sectors.*

Proof. Let u_0 be the representation vector field for f. Write $z = a + re^{i\theta}$. The estimate (4) gives

$$u_0(z) = \alpha e^{id\theta} + o(r) \qquad \text{for } \theta \in [0, 2\pi). \tag{8}$$

Writing $\alpha = e^{i\theta_0/N}$, the Nth-roots of the $u_0(z)$ are then given by $e^{i(\frac{d\theta+\theta_0}{N} + \frac{2\pi k}{N})}$ for $k \in \mathbb{Z}$.

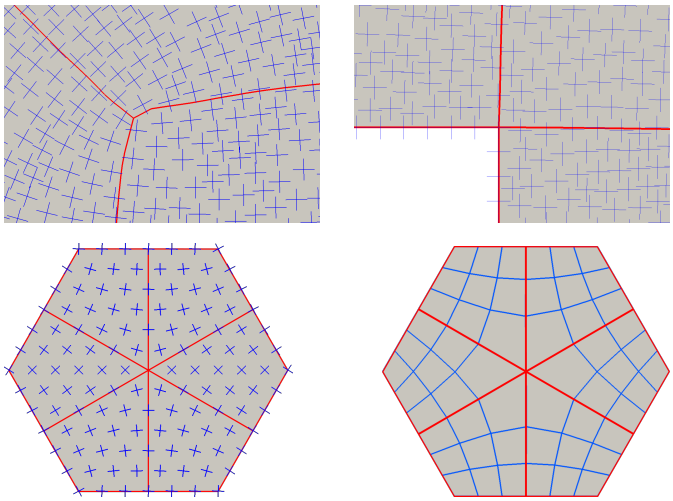

FIG. 7. **(top)** *Local behavior of cross fields around an interior singularity (***left***) and boundary singularity (***right***). The thick red lines show the separatrices exiting singularities as described by Lemmas 5.1 and 5.4. If the separatrices are considered as boundaries of the sectors, then the index of each corner is* $+1/4$*; see Definition 5.3.* **(bottom left)** *A cross field and speparatrix partition for a regular hexagon. The singularity in the center has index* $-1/2$*.* **(bottom right)** *The corresponding quad mesh with skeleton highlighted in red; see Definition 3.7.*

We seek directions where the vector originating at a and pointing towards z is parallel to a vector originating at the origin and pointing towards any of the N*th*-roots. Thus we want to solve the equation

$$e^{i\theta} = e^{i(\frac{d\theta+\theta_0}{N}+\frac{2\pi k}{N})} \quad \Longrightarrow \quad \theta = 2\pi k/(N-d) + \theta_0/(N-d) \tag{9}$$

Since we are looking for solutions where $\theta \in [0, 2\pi)$ we have exactly $N - d$ solutions. This gives $N - d$ separatrices and $N - d$ sectors. ∎

5.2. Boundary singularities and nearby behavior of canonical harmonic N-direction fields. We can make further assertions about the behavior of N-direction fields on these sectors, but first we must introduce the concept of boundary singularities:

DEFINITION 5.2. *Let ∂D be piecewise smooth with corners $\{c_1, \ldots, c_k\}$. Let $\operatorname{int}(c_i)$ be the interior angle at the corner c_i. The* angle of deviation *at a corner c_i is the signed angle $\operatorname{dev}(c_i) = \pi - \operatorname{int}(c_i)$.*

DEFINITION 5.3. *Let ∂D be piecewise smooth with corners $\{c_1, \ldots, c_k\}$. Let $\gamma\colon [0,1] \to \overline{D}$ be a simple closed curve such that $\gamma(0) = c_i = \gamma(1)$, and $y'(0)$ and $y'(1)$ are tangent to ∂D at c, and containing no other singularity. Let*

$$\Delta \arg(c_i) = \lim_{s \downarrow 0} \arg R(f(\gamma(1-s))) - \arg R(f(\gamma(s))).$$

The index *of the corner is defined*

$$\mathrm{I}(c_i) \coloneqq \frac{\operatorname{dev}(c_i) - \frac{1}{N}\Delta \arg(c_i)}{2\pi}. \tag{10}$$

The corner c_i is said to be a boundary singularity *if its index is non-zero.*

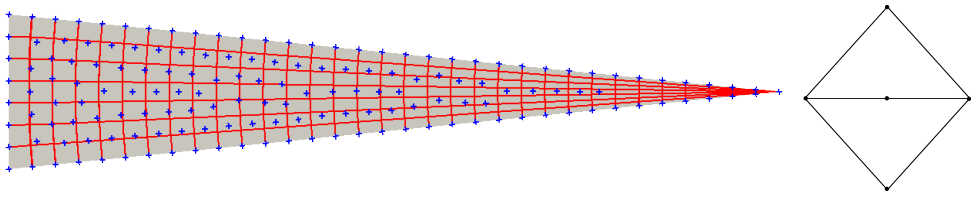

FIG. 8. *Singularities of index* $\geq 1/2$ *lead to degenerate quad meshes.* **(left)** *A boundary singularity of index* $1/2$ *leads to an infinite number of separatrices converging to a single point.* **(right)** *An internal singularity of index* $1/2$ *leads to a pair of the degenerate "doublet" quads.*

A boundary singularity can be interpreted as the number of $1/N$ turns in the counterclockwise direction that the N-direction makes in relation to the boundary. It is akin to the concept of a *turning number* from [37], except that it happens at a single point (see Figure 4).

To apply the Ginzburg-Landau theory to a domain D with corners, we first smooth the corners via the operation described in section 3 and Figure 4, to obtain a canonical harmonic N-direction field $\widetilde{f}$ defined on a smooth domain $\widetilde{D}$. We then extend $\widetilde{f}$ to D constant along each ray from the corner; see Figure 4.

LEMMA 5.4. *Let* N *be even and* f *as described in the previous paragraph. Let* c *be a boundary singularity of* f *of index* d/N *with* $d < N/2$*. There are exactly* $\frac{N}{2} - d + 1$ *separatrices meeting at* c_j *(including the boundaries themselves). These separatrices partition a neighborhood of* c *into* $\frac{N}{2} - d$ *even-angled sectors.*

Proof. Let $\phi_c = \text{int}(c)$. By the definition of a boundary singularity (Definition 5.3), we calculate that $\Delta \arg(c) = N(\pi - \phi_c) - 2\pi d$. We can parameterize the geometry near the corner with polar coordinates (r, ϕ), where r is the distance between from the corner and $\phi \in [0, \phi_c]$ measures the angle from the segment succeeding the corner. In this coordinate system, the representation field, u, near the corner can be written

$$u = e^{-i\phi \frac{\Delta \arg(c)}{\phi_c}} = e^{-i\phi \frac{N(\pi - \phi_c) - 2\pi d}{\phi_c}}. \tag{11}$$

Just as in Lemma 5.1, we want to find any rays emanating from the singularity such that the crosses along those rays are aligned with the rays. Thus, we want to solve

$$e^{i\phi} = e^{-i\phi \frac{N(\pi - \phi_c) - 2\pi d}{N\phi_c} + \frac{2\pi k}{N}} \quad \Longrightarrow \quad \phi = \frac{\phi_c}{\frac{N}{2} - d} k. \tag{12}$$

Since we are looking for solutions in $\phi \in [0, \phi_c]$, for $d < N/2$ and N even we have solutions for $k = 0, \ldots, \frac{N}{2} - d$. Thus the N-direction field corresponding to u partitions a neighborhood of the corner into $\frac{N}{2} - d$ even-angled sectors. ∎

In Lemma 5.4, if we allow $d = N/2$ then (12) simplifies to the identity, and so for every value of θ we get a separatrix. In the case of a cross field, this means that any boundary singularity with index $+1/2$ has infinitely many separatrices; see Figure 8 (left).

The following Lemma specifies the behavior of the cross field within each sector around a singularity.

LEMMA 5.5. *Let* N *be even and* $d < N/2$*. Consider a component of the partition described in Lemmas 5.1 and 5.4. A singularity,* c*, in the corner of this component, when viewed as a boundary singularity, has index* $\frac{1}{2} - \frac{1}{N}$*.*

Proof. If the singularity is an internal singularity, then (9) gives that on each of the sectors, the angle of deviation is

$$\operatorname{dev}(c) = \pi - \left(\left[\frac{2\pi(k+1)}{N-d} + \frac{\theta_0}{N-d} \right] - \left[\frac{2\pi k}{N-d} + \frac{\theta_0}{N-d} \right] \right) = \pi - \frac{2\pi}{N-d}.$$

From (8), we compute

$$\begin{aligned} -\Delta \arg(c) &= d \left[\frac{2\pi(k+1)}{N-d} + \frac{\theta_0}{N-d} \right] + \theta_0 - \left(d \left[\frac{2\pi k}{N-d} + \frac{\theta_0}{N-d} \right] + \theta_0 \right) \\ &= d \frac{2\pi}{N-d}. \end{aligned}$$

Using (10), the index of the corner is

$$\mathrm{I}(c) = \frac{\pi - \frac{2\pi}{N-d} - \frac{d}{N} \frac{-2\pi}{N-d}}{2\pi} = \frac{\frac{N}{2} - 1}{N}.$$

If the singularity is a boundary singularity, then from eq. (12), the angle of deviation for each sector is

$$\operatorname{dev}(c) = \pi - \left(\left[\frac{\phi_c(k+1)}{\frac{N}{2} - d} \right] - \left[\frac{\phi_c k}{\frac{N}{2} - d} \right] \right) = \pi - \frac{\phi_c}{\frac{N}{2} - d}.$$

Using (11), we compute

$$\Delta \arg(c) = \frac{N(\pi - \phi_c) - 2\pi d}{\phi_c} \left(\frac{\phi_c(k+1)}{\frac{N}{2} - d} - \frac{\phi_c k}{\frac{N}{2} - d} \right) = \frac{N(\pi - \phi_c) - 2\pi d}{\frac{N}{2} - d}.$$

Thus (10) gives that the index of the corner is

$$\mathrm{I}(c) = \frac{\pi - \frac{\phi_c}{\frac{N}{2} - d} - \frac{1}{N} \frac{N(\pi - \phi_c) - 2\pi d}{\frac{N}{2} - d}}{2\pi} = \frac{\frac{N}{2} - 1}{N}. \qquad \square$$

Lemma 5.5 says that the index of the boundary singularity around the corner of any sector is $(\frac{N}{2} - 1)/N$. When $N = 4$, this simply means that each corner of a sector looks like a right angle with respect to the cross field; see Figure 7. Thus locally, the neighborhood of an internal singularity of index d/N has the same structure as an irregular node of a quad mesh of valence $N - d$; see Figure 7 (bottom).

The next section shows how we can use this local structure to determine the structure of a quad mesh on D.

5.3. Partitioning into four-sided regions. The skeleton of a quad mesh (Definition 3.7) gives the basic structure of the mesh in the sense that it partitions the domain into the coarsest possible quad layout for the given choice of irregular nodes and connectivity between them; see Figure 2 (bottom), Figure 7 (bottom left), and Figure 11 (right). Any mesh with this structure, including the original mesh, can be seen as simply a refinement of this quad layout.

It is well known that a cross field can be generated on a quad mesh by locally aligning the crosses with quad edges (see [3, 49]). Beaufort et al. [3] show that a cross field created in such a way will have singularities exactly at the irregular nodes. Further, the separatrices of the cross field will be exactly the curves traced out by the

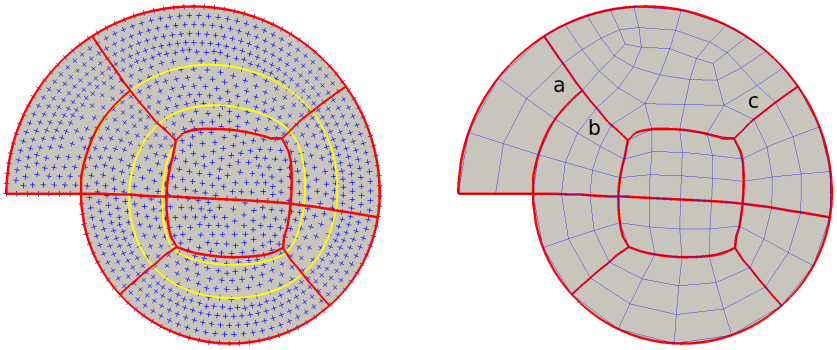

FIG. 9. *A cross field on a domain that exhibits a limit cycle.* **(left)** *The separatrix traced in yellow converges to a limit cycle. The partition shown in red inserts a T-junction at the first place where the yellow separatrix intersects another one.* **(right)** *The four-sided regions without a T-junction can be meshed by conformal mapping. The region with the T-junction requires the insertion of more irregular nodes in order to conform with the mesh on its right and left sides.*

skeleton of the quad mesh. Presumably, one could create the skeleton of a quad layout by reversing this process, *i.e.*, simply tracing separatrices of the cross field (this is the approach taken in [21]). This would allow for meshing the domain by conformally mapping a regular grid into each region of the quad layout. Unfortunately, it is not always so simple. Figure 9 shows a geometry that contains a limit cycle. The yellow separatrix begins at the corner, but continues indefinitely as it approaches the limit cycle. The following theorem shows that this is the only type of failure case that can occur. The second part of the proof follows [29].

THEOREM 5.6. *Let f be a boundary-aligned canonical harmonic cross field on D whose singularities have index $\leq 1/4$. If no separatrix of f converges to a limit cycle, then the separatrices of f, along with ∂D partition D into a quad layout.*

Proof. By Lemma 5.1, a finite number of separatrices meet at each singularity. Since no separatrix converges to a limit cycle on D (and consequently, none on $\mathcal{R}$) the Poincaré-Bendixson theorem for manifolds [41] guarantees that each separatrix must either end at another singularity, or exit the domain orthogonal to the boundary. The set of separatrices along with ∂D then partition the domain into bounded regions that contain no singularities. If a curve of the boundary of any region meets another curve, the corner where they meet must have index $+1/4$ because they are either separatrices intersecting each other or the boundary orthogonally, or they meet at singularities and by Lemma 5.5 have index $+1/4$. Since there are no internal singularities, the total index must come from corner singularities, and since the index for each corner is positive, the sum must be non-negative. By the Poincaré-Hopf theorem for cross fields [37], the total index of a given region must equal the Euler characteristic of that region. The genus of each region is zero because the domain is defined in two dimensions. Thus there are only two possibilities; either there is one boundary and the Euler characteristic is one, in which case we have four corners each of index $+1/4$, a quad element. Otherwise, there are two boundaries and the Euler characteristic is zero. In this case the total index is zero, so there are no singularities, *i.e.*, an annulus. □

The main takeaway is that when no separatrix of the cross field converges to a limit cycle, the topology of the cross field is sufficient to uniquely determine a quad layout, which can then easily be meshed by mapping a regular grid into each

region. The irregular nodes of any such mesh mirror exactly the singularity structure of the cross field through the relationship established in Lemmas 5.1 and 5.4. Further, since the index of each singularity is $\leq 1/4$, each singularity will have at least three separatrices, and so none of the quad elements of the mesh will be degenerate; see Figure 8.

The failure case occurs when one of the separatrices converges to a limit cycle. In a case like this, we propose that such separatrices can easily be handled by allowing T-junctions on the quad layout; see Figure 9. This complicates the meshing problem slightly; a domain can no longer be meshed by simply mapping a regular grid into each region of the quad layout. Instead, regions adjacent to T-junctions will require additional singularities to resolve the differing number of quads needed on opposite sides of the region. This however has been addressed in [40, 45, 46], and so partitioning the domain into a quad layout with T-junctions is sufficient to produce a quad mesh where the number, location, and valence of its irregular nodes are determined only by the singularities and T-junctions in the partition, and the target density of the quad mesh. See subsection 6.2 for more details.

THEOREM 5.7. *Let f be a smooth cross field on D with a finite singularity set. Every separatrix that converges to a limit cycle intersects at least one other separatrix.*

Proof. Let $s\colon [0,\infty) \to D$ be a separatrix beginning at a singularity $s(0)$ with $s(t)$ converging to the limit cycle, γ_∞, as $t \to \infty$. Since s converges to γ_∞, there exists a t^* such that a streamline intersecting s at $s(t^*)$ must also intersect γ_∞. Let $s^+_{\perp,t^*}$ be the segment of this streamline beginning at $s(t^*)$ and continuing in the direction towards γ_∞. Consider the the family of streamline segments $s^+_{\perp,t}$ for $t \in [0,\infty)$ beginning at $s(t)$, and continuing in the direction from s consistent with $s^+_{\perp,t^*}$. Let this family of curves be parameterized so that each curve, $s^+_{\perp,t}(r)$, has unit speed and starts on s at $s(t)$ when $r = 0$. Finally, let $s_{\perp,t}$ be the corresponding streamlines.

If $s^+_{\perp,t}$ intersects γ_∞, for every t, then $s^+_{\perp,0}$ must also be a separatrix (since it starts at a singularity), and since it intersects γ_∞ it must also intersect s. If $s^+_{\perp,t}$ does not intersect γ_∞, for all t, then there is a greatest lower bound, τ, such that for $t > \tau$, $s^+_{\perp,t}$ must intersect γ_∞.

We claim that $s^+_{\perp,\tau}$ cannot intersect γ_∞. If it did, then by the stability of ordinary differential equations with respect to initial data, [10, Proposition 2.76], there would be a neighborhood around $s(\tau)$ within which any streamline would also intersect γ_∞, contradicting the fact that τ is a greatest lower bound.

We claim that $s^+_{\perp,\tau}$ connects to a singularity, making $s_{\perp,\tau}$ a separatrix, and argue by contradiction. If $s^+_{\perp,\tau}$ does not connect to a singularity, then by the Poincaré-Bendixson theorem, either $s_{\perp,\tau}$ is a periodic orbit (case 1), or $s^+_{\perp,\tau}$ will exit the boundary (case 2) or approach a limit cycle (case 3).

Case 1: If $s_{\perp,\tau}$ is a periodic orbit, then since both $s_{\perp,\tau}$ and γ_∞ are closed sets, there is a finite distance, $\delta > 0$, between $s_{\perp,\tau}$ and γ_∞. Let $V = \{x \in D\colon d(x, s_{\perp,\tau}) < \delta/2\}$. By [10, Proposition 2.76], there exists an $\varepsilon > 0$ such that $s^+_{\perp,t}$ must remain in V for $t \in (\tau - \varepsilon, \tau + \varepsilon)$. Then $s^+_{\perp,\tau+\varepsilon/2}$ must remain in V, and on the other hand, must intersect γ_∞ since $\tau + \varepsilon/2 > \tau$. This is a contradiction since $V \cap \gamma_\infty$ is empty.

Case 2: Suppose that $s^+_{\perp,\tau}$ exits the boundary. Since $s^+_{\perp,\tau}$ and γ_∞ are a compact sets, there exists a $\delta > 0$ such that the set $V = \{x \in D\colon d(x, s^+_{\perp,\tau}) < \delta/2\}$ has an empty intersection with γ_∞. Again by [10, Proposition 2.76] there is an $\varepsilon > 0$ such that $s^+_{\perp,t}$ must remain in V for all $r \geq 0$ when $t \in (\tau-\varepsilon, \tau+\varepsilon)$. But $s^+_{\perp,t+\varepsilon/2}$ intersects

γ_∞, which again is a contradiction since $V \cap \gamma_\infty$ is empty.

Case 3: Suppose $s^+_{\perp,\tau}$ approaches a limit cycle ℓ_∞. Then there exists an r^* and an $\varepsilon_1 > 0$ such that if $t \in (\tau-\varepsilon_1, \tau+\varepsilon_1)$, then $s^+_{\perp,t}(r)$ approaches ℓ_∞ asymptotically as r increases from r^* to ∞. Consider the segment of $s^+_{\perp,\tau}(r)$ for $r \in [0, r^*]$. This segment is a closed set, so again there is a δ such that the set $V = \{x \in D\colon d(x, s^+_{\perp,\tau}(r)) < \delta/2 \text{ for } r \in [0, r^*]\}$ has an empty intersection with γ_∞. Again, by [10, Proposition 2.76], there is a $\varepsilon_2 > 0$ such that $s^+_{\perp,t}$ must remain in V for all $r \in [0, r^*]$ when $t \in (\tau-\varepsilon_2, \tau+\varepsilon_2)$. Let $\varepsilon = \min(\varepsilon_1, \varepsilon_2)$. Then for $t \in (\tau-\varepsilon, \tau+\varepsilon)$, $s_{\perp,t}+(r) \in V$ for $r < r^*$, and approaches ℓ_∞ asymptotically afterwards. Thus $s^+_{\perp,t+\varepsilon/2}$ cannot intersect γ_∞, which again is a contradiction. ∎

COROLLARY 5.8. *Let f be as in Theorem 5.7. Let γ_∞ be a limit cycle with a separatrix, s, converging to it. There is a separatrix, s', (not necessarily the same as s) that converges to γ_∞ that also intersects a separatrix beginning at the same singularity.*

Proof. Let $s_{\perp,t}$ be defined as in Theorem 5.7. Either $s_{\perp,t}$ intersects γ_∞ for all t (case A), or not (case B). In case A, by Theorem 5.7 s intersects $s_{\perp,0}$, which is a separatrix beginning at the same singularity, so $s' = s$ and we are done. In case B, by Theorem 5.7, $s^+_{\perp,t}$ connects to a singularity at some time. Denote the time by $t = \tau$, the singularity by x_τ, and the separatrix by $s^+_{\perp,\tau}$.

For some sufficiently small $\varepsilon > 0$, consider the segment of $s^+_{\perp,\tau+\varepsilon}$ beginning at $s(\tau+\varepsilon)$ and terminating at its first intersection with γ_∞. Call this segment $s^*_{\perp,\tau+\varepsilon}$. Since s converges to γ_∞, for any point p on $s^*_{\perp,\tau+\varepsilon}$, s will always intersect $s^*_{\perp,\tau+\varepsilon}$ between p and γ_∞. Thus all streamlines intersecting $s^*_{\perp,\tau+\varepsilon}$ must converge to γ_∞. One of these must be a separatrix connecting to x_τ since s and γ_∞ are on opposite sides of x_τ. This new separatrix must fall into case A or case B. If it falls into case A we are done. If it falls into case B, then by repeating this argument we can always find another separatrix converging to γ_∞. Since there are only a finite number of singularities, we can only repeat this process a finite number of times until eventually finding a limit cycle that falls into case A. ∎

Theorem 5.7 and Corollary 5.8 allow us to deal with the issue of limit cycles in a predictable manner. When a limit cycle occurs in the cross field, the partition can be obtained by first tracing out all of the separatrices that don't converge to a limit cycle, and then tracing out each separatrix that does converge to a limit cycle until it reaches another separatrix, placing a T-junction at that point. The exact process for partitioning a domain into a quad layout with T-junctions is specified in Algorithm 1. We denote the set of separatrices that converge to any limit cycle by $\mathcal{P}$.

THEOREM 5.9. *Algorithm 1 is well defined, terminates in finite time, and partitions D into a quad layout with exactly $|\mathcal{P}|$ T-junctions.*

Proof. The first 'for' loop is well-defined by Corollary 5.8.

In the second 'for' loop, each separatrix that converges to a limit cycle is guaranteed to intersect another separatrix by Theorem 5.7. If it does not intersect a separatrix in $\mathcal{S}$, then it must intersect one that runs orthogonal to the limit cycle itself which is added to $\mathcal{B}$ in the first for loop.

Clearly Algorithm 1 partitions the domain into regions without singularities. As in Theorem 5.6, each corner formed by the partitioning must have an index of 1/4 because it either meets at a singularity, intersects another separatrix, or exits the boundary orthogonally. Following the argument from the second part of the proof of

Algorithm 1 Partitioning D into a quad layout with T-junctions.

Input: Let D be a domain satisfying Assumption 3.1. Let f be a boundary-aligned canonical harmonic cross field for a given set of singularities.

Output: A set $\mathcal{B}$ containing limit cycles and separatrices that define a quad layout with T junctions.

Let $\mathcal{S}$ be the set of separatrices that do not converge to a limit cycle. Let $\mathcal{P}$ be the set of separatrices that do. Let $\mathcal{L}$ be the set of limit cycles.

Initialize the set $\mathcal{B} = \mathcal{S}$.

for $l \in \mathcal{L}$ **do**
  if no element of $\mathcal{B}$ intersects l **then**
    (i) Add l to $\mathcal{B}$.
    (ii) By Corollary 5.8, there is an element of $\mathcal{P}$ that intersects l. Let ρ' be the portion of that separatrix beginning at the singularity and ending in a T-junction with l.
    (iii) Add ρ' to $\mathcal{B}$.
    (iv) remove ρ from $\mathcal{P}$.
  end if
end for
for $\rho \in \mathcal{P}$ **do**
  Let ρ' be the curve segment of ρ beginning at the singularity and continuing until it intersects an element of $\mathcal{B}$. Add ρ' to $\mathcal{B}$.
end for

Theorem 5.6, this is enough to guarantee that each region is a quad or an annulus. There are exactly $|\mathcal{P}|$ T-junctions because they are created exactly when we trace a separatrix in $|\mathcal{P}|$ until it reaches another separatrix that is already in the set $\mathcal{B}$. ∎

6. Computational methods.

6.1. The MBO method. Another consequence of the connection between the cross field design problem and Ginzburg-Landau Theory is an efficient computational method for minimizing the Ginzburg Landau functional (3) based on a generalization of the Merriman-Bence-Osher (MBO) method. The MBO method was originally introduced in [25, 26, 27] in the context of diffusion generated motion by mean curvature and extended to (3) in [39]. The details of the algorithm are given in Algorithm 2. We view this method as an energy splitting method for the Ginzburg-Landau functional (3) where we alternatively (i) diffuse the representation map by a time τ and (ii) project onto the unit circle. The intuition behind Algorithm 2 is that the Dirichlet energy of a representation map decreases in the first step, as it is the gradient flow of the Dirichlet energy subject to the boundary condition. In the second step, the representation map is projected on $\mathbb{T}$.

The MBO method (Algorithm 2) provides an efficient way to approximate local minimizers for the Ginzburg-Landau energy (3). By subsection 4.1. local minimizers will have isolated singularities of degree ± 1. The field produced by Algorithm 2 is a boundary-aligned canonical harmonic map for some singularity configuration, so the results in section 5 apply, and Theorems 5.6 and 5.9 guarantee that its separatrices will partition the domain into four-sided regions.

Algorithm 2 A diffusion generated motion algorithm for approximating minimizers of the Ginzburg-Landau energy (3).

Input: Let D be a domain satisfying Assumption 3.1 and $\tau > 0$. Fix boundary conditions g on ∂U as in Definition 3.12. Initialize a representation map of the cross field, $u_0 \colon D \to \mathbb{C}$, with $u_0(x) = g(x)$ for every $x \in \partial D$. Let $k = 0$.

while the u_k is not stationary **do**

(i) Solve the diffusion equation,

$$\partial_t v(t,x) = \Delta v(t,x) \qquad x \in D \tag{13a}$$

$$v(t,x) = g(x) \qquad x \in \partial D \tag{13b}$$

$$v(0,x) = u_k(x) \qquad x \in D, \tag{13c}$$

until time τ. Denote the solution by $\tilde{u}_{k+1} = e^{\tau\Delta} u_k = v(\tau)$.

(ii) Set $u_{k+1} = \frac{\tilde{u}_{k+1}}{|\tilde{u}_{k+1}|}$ and $k = k + 1$.

end while

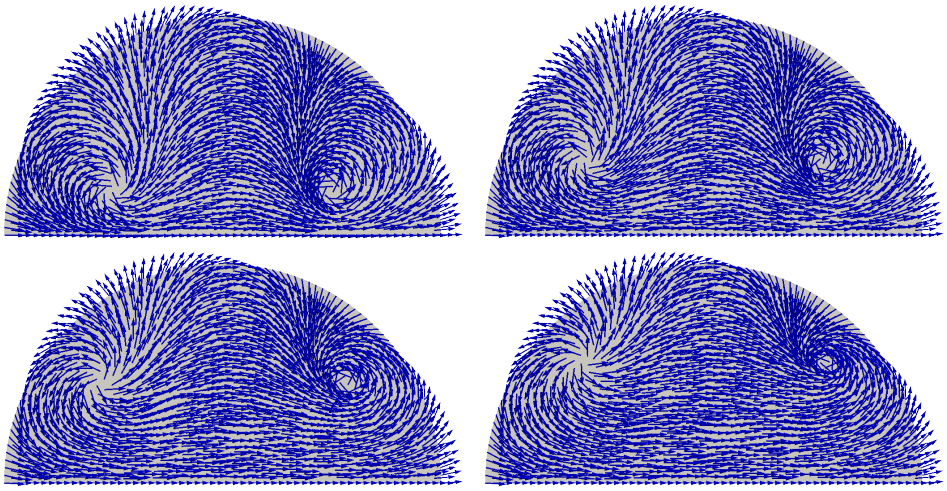

FIG. 10. *Iterations 0, 1, 3, and 19 of Algorithm 2 for a half disk. At each time step, the representation field is drawn. As time evolves the singularities in the field move as to reduce the Ginzburg-Landau energy (3). The time step in Algorithm 2, τ, was chosen very small so that the algorithm takes several steps to reach a stationary state.*

Given a domain D, we discretize it with linear triangle elements, and assign a Dirichlet boundary condition at each boundary node. We initialize the field either with a canonical harmonic map using Theorem 4.3, or with a harmonic map obtained by solving Laplace's equation on D. The diffusion steps of the MBO iterations are then performed with a finite element method using the FEniCS software [2].

6.2. Creating a quad mesh from a representation field. The discrete representation map produced by our implementation of the MBO method can be transformed into a discrete cross field by taking the fourth root of the representation map at any point. Singularities occur at the zeros of the representation map. The direc-

tions that separatrices exit a singularity are then computed by using (9) and (12), and separatrices are computed using a fourth order Runge-Kutta method. There is no need to compute a Riemann surface for the domain for streamline tracing because locally the appropriate vector field is completely determined.

By tracing out streamlines as specified in Algorithm 1, we obtain a partition of the domain into a quad layout with exactly one T-junction for every separatrix that approaches a limit cycle. For quad layouts that contain no T-junctions, a regular grid can be conformally mapped into each quad region to obtain the mesh. We do this using the CUBIT software [40].

When a T-junctions appears in a quad layout, a mesh can no longer be obtained by simply mapping a grid into each region. The problem is illustrated in Figure 9 (right). To mesh a region, the opposite sides of that region must have the same number of quads. If we were to map a regular grid into each subsequent region, we would have to satisfy the conditions $a + b = c$, $c = b$, $a > 0$, $b > 0$ and $c > 0$ where a and b are the number of quads required on the sides adjacent to the T-junction, and c is the number of quads required on the opposite side; see Figure 9. Clearly these conditions are incompatible, so any mesh in such a region will require additional singularities. In our examples, we mesh these regions using the paving algorithm [5], however a more deterministic method such as [46] could be used.

These singularities do not necessarily need to be placed in the region adjacent to the T-junction as shown in Figure 9, but can be distributed throughout the regions by assigning the number of quads to appear on each curve. This is a combinatorial problem similar to the user specified interval assignment problem considered in [28].

Figure 11 shows several example meshes using this method. The first example is a surface from a CAD designed mechanical part [40]. This domain has Brouwer degree two and the cross field contains two singularities of index $+1/4$. Three separatrices meet at each of these singularities, and thus the corresponding quad mesh has 3-valent nodes at the singularity locations.

The second example is a block U. The field was initialized with a canonical harmonic cross field with a boundary condition of Brouwer degree -2 and a singularity configuration placing two singularities of index $-1/4$ in the bottom corners of the U. The corresponding quad mesh has two 5-valent nodes.

The next two examples are multiply connected domains. As stated in section 3, these examples could be handled within the framework of this paper by cutting the domain, however in practice we apply the MBO method directly to the multiply connected domain. The first multiply connected domain has Brouwer degree -1, which we count by subtracting the Brouwer degree of the interior boundaries from the exterior one. One singularity of index $-1/4$ appears near the curve that contributes to the negative Brouwer degree. The cross field in the last example contains two singularities with index $-1/4$, and also contains periodic orbits that intersect themselves.

7. Discussion and future directions. In this paper, we have made the observation that cross field design for two-dimensional quad meshing is related to the well-known Ginzburg-Landau problem from mathematical physics. Using this identification, we prove that this procedure can be used to produce a cross field whose separatrices partition the domain into four sided regions. This identification also allows for an extension of the Merriman-Bence-Osher (MBO) threshold dynamics method to be used to find representation fields that approximately minimize the Ginzburg-Landau energy. The methods are demonstrated with a number of computational examples.

Some limitations exist when using the energy (1). Since the problem is non-

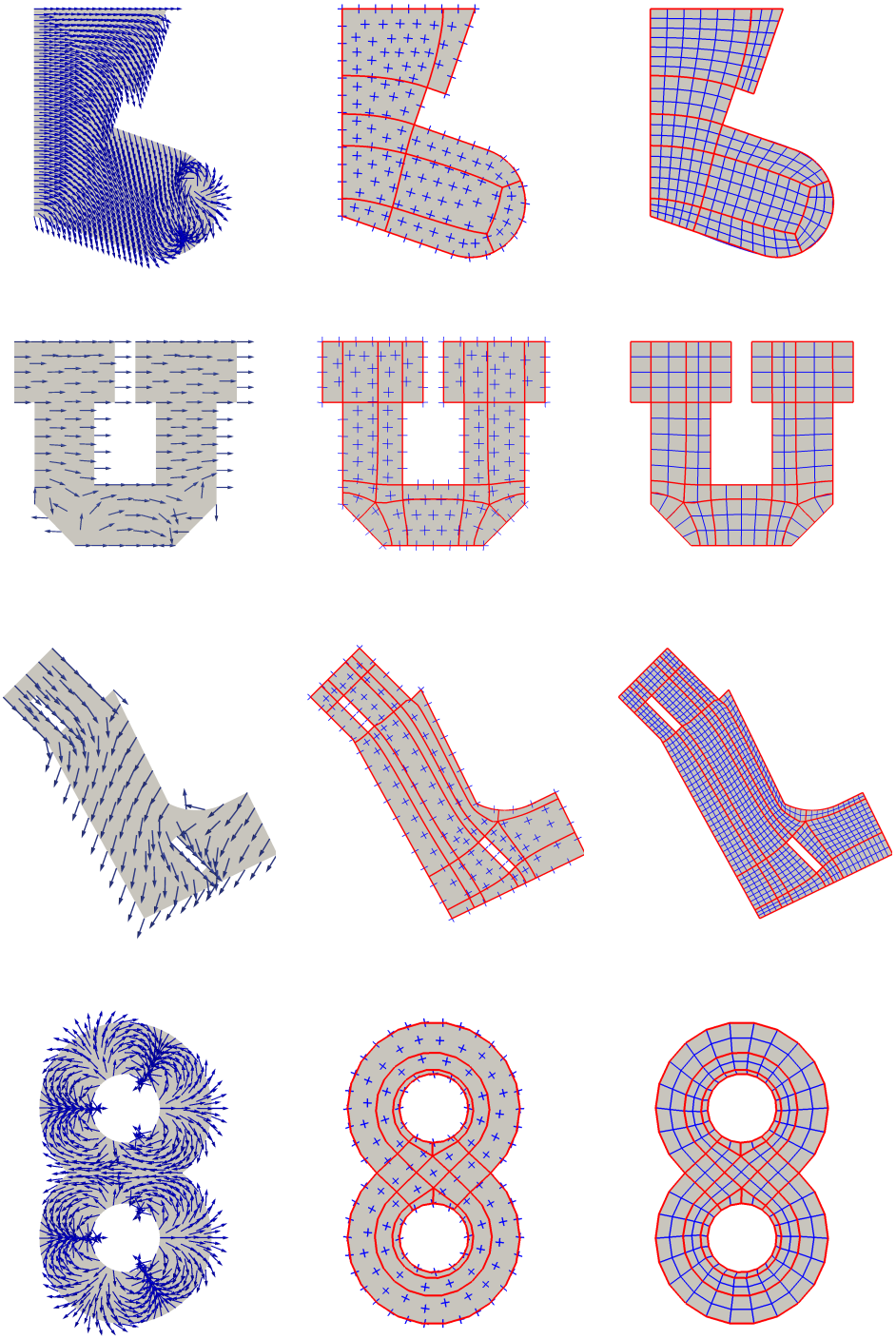

FIG. 11. *For several different geometries (rows), we plot the* **(left)** *representation field obtained via the MBO method (Algorithm 2),* **(center)** *the cross field and quad layout obtained from the separatrices of the cross field, and* **(right)** *quad mesh with skeleton drawn in red.*

convex, for most domains, we cannot guarantee that we will reach a global minimum. Ironically, a global minimum may not always result in the best mesh. For example, the cross field in Figure 6 (left) is the global minimizer of the Ginzburg-Landau energy for this domain because it is the canonical harmonic cross field with no singularities. The one shown in Figure 6 (center) is the cross field obtained through the MBO method. Isotropy of mesh elements is a desirable property in many meshing applications, and in this case the local minimizer found by the MBO method produces a more isotropic mesh than the global minimizer because of the additional singularities. This suggests that this definition of cross field energy may assign too much weight to singularities. The infinite energy at singularities is also problematic because the discrete measure of field energy depends on the discretization. As the mesh is refined near singularities, the energy is increased.

Despite these limitations, we have shown that approximate solutions to problem (1) has many desirable properties for meshing. For example, the MBO method produces cross fields with isolated singularities of index $\pm 1/4$ (subsection 4.1) that locally exhibit the same structure as irregular mesh nodes subsection 5.1. Further, the separatrices of these cross fields are guaranteed to partition a domain into a quad layout, possibly with T-junctions.

There are a number of future directions for this work. One direction is a more careful numerical analysis of the finite element problem arising in the discretization of (3). Along the same line, a more careful comparison should be made with the quad meshing methods in [15, 16, 18, 21, 33]. Also, a comparison between the location of singularities of fields generated via this method and those generated via the method in [18], utilizing a different cross field energy, is necessary.

In section 3 we discuss a method to smooth the corners of a piecewise smooth domain so as to be able to apply the Ginzburg-Landau theory. A more elegant solution would be to extend the Ginzburg-Landau theory to handle domains with piecewise smooth boundary.

In this paper, the index of a boundary singularity is determined by the corner smoothing operation in section 3. While this is a natural choice, it does not allow us to mesh geometries with sharp corners such as that in Figure 8 (left), since a boundary singularity of index $1/2$ would be assigned. While quad elements are more isotropic when the index values are chosen close to $\mathrm{dev}(c)/2\pi$, in reality, there is ambiguity in the index assignment of any corner. For example, the bottom four corners on the block U in Figure 11 were each assigned an index of $1/4$, but an index of zero would have been just as reasonable, and would change the resulting cross field and mesh. It may be preferable to let the user have control of the index assignment for each corner to allow for greater flexibility for the mesh and enable meshing of geometries with sharp corners.

Proving general symmetry results for solutions of the Ginzburg-Landau energy is a difficult problem. In [23], a the symmetric solution on a disc is analyzed and is shown to be stable under perturbations. See also [9] for further discussion and open problems. However, we observe in numerous numerical examples that the symmetries of a domain are inherited by the configuration of the Ginzburg-Landau vortices. Analytical results in this direction *for the specific boundary conditions considered here* could be used to guarantee symmetries in the resulting mesh.

For simplicity, in this paper we have restricted to *planar Euclidean domains* and not *surfaces* with boundary. However, due to the topological nature of our results and the Ginzburg-Landau Theory, we expect that many of these results can be extended to surfaces [43]. We also intend to extend our implementation of the MBO method to

surfaces, as well as a generalization of the method discussed in section 4 for producing fields with a fixed set of singularities.

In higher dimensions, the analogous approach is to minimize the Dirichlet energy over the set of H^1 functions taking values in $SO(3)/O$ where O is the octahedral symmetry group [14, 35, 42]. Unfortunately, this approach is more complicated as the field topology is no longer sufficient to determine the underlying structure of a hex mesh [48]. Finding an efficient representation for elements of the set $SO(3)/O$ and studying the singularity structure for generalized solutions of this problem requires further attention.

Acknowledgments. We would like to thank Dan Spirn and Matthew Staten for helpful discussions and comments, and Franck Ledoux for providing access to the GMDS meshing library.

REFERENCES

[1] P. Alliez, D. Cohen-Steiner, O. Devillers, B. Lévy, and M. Desbrun, *Anisotropic polygonal remeshing*, in ACM SIGGRAPH 2003 Papers, SIGGRAPH '03, ACM, 2003, pp. 485–493, https://doi.org/10.1145/1201775.882296.

[2] M. Alnæs, J. Blechta, J. Hake, A. Johansson, B. Kehlet, A. Logg, C. Richardson, J. Ring, M. E. Rognes, and G. N. Wells, *The FEniCS project version 1.5*, Archive of Numerical Software, 3 (2015), https://doi.org/10.11588/ans.2015.100.20553.

[3] P.-A. Beaufort, J. Lambrechts, F. Henrotte, C. Geuzaine, and J.-F. Remacle, *Computing two dimensional cross fields - a PDE approach based on the Ginzburg-Landau theory*, in Proceedings of the 21st International Meshing Roundtable, Elsevier Ltd., 2017, https://arxiv.org/abs/1706.01344.

[4] F. Bethuel, H. Brezis, and F. Hélein, *Ginzburg-Landau Vortices*, vol. 13 of Progress in Nonlinear Differential Equations and Their Applications, Birkhäuser Boston, 1994, https://doi.org/10.1007/978-1-4612-0287-5.

[5] T. D. Blacker and M. B. Stephenson, *Paving: A new approach to automated quadrilateral mesh generation*, International Journal for Numerical Methods in Engineering, 32 (1991), pp. 811–847, https://doi.org/10.1002/nme.1620320410.

[6] D. Bommes, M. Campen, H.-C. Ebke, P. Alliez, and L. Kobbelt, *Integer-grid maps for reliable quad meshing*, ACM Trans. Graph., 32 (2013), art. 98, pp. 1–12, https://doi.org/10.1145/2461912.2462014.

[7] D. Bommes, B. Lévy, N. Pietroni, E. Puppo, C. Silva, M. Tarini, and D. Zorin, *Quad meshing*, Eurographics 2012 State of the Art Reports, (2012), https://doi.org/http://dx.doi.org/10.2312/conf/EG2012/stars/159-182.

[8] D. Bommes, H. Zimmer, and L. Kobbelt, *Mixed-integer quadrangulation*, in ACM SIGGRAPH 2009 Papers, SIGGRAPH '09, ACM, 2009, pp. 1–10, https://doi.org/10.1145/1576246.1531383.

[9] H. Brezis, *Symmetry in nonlinear PDEs*, in Proceedings of Symposia in Pure Mathematics, vol. 65, American Mathematical Society, 1999, https://doi.org/http://dx.doi.org/10.1090/pspum/065.

[10] C. Chicone, *Ordinary Differential Equations with Applications*, Texts in Applied Mathematics, Springer, New York, Berlin, Heidelberg, 2 ed., 2006, http://www.springer.com/us/book/9780387307695.

[11] K. Crane, M. Desbrun, and P. Schröder, *Trivial connections on discrete surfaces*, Computer Graphics Forum, 29 (2010), pp. 1525–1533, https://doi.org/10.1111/j.1467-8659.2010.01761.x.

[12] O. Diamanti, A. Vaxman, D. Panozzo, and O. Sorkine-Hornung, *Designing n-PolyVector fields with complex polynomials*, in Computer Graphics Forum, vol. 33, Wiley Online Library, 2014, pp. 1–11, https://doi.org/10.1111/cgf.12426.

[13] A. Hertzmann and D. Zorin, *Illustrating smooth surfaces*, in Proceedings of the 27th Annual Conference on Computer Graphics and Interactive Techniques, SIGGRAPH '00, ACM Press/Addison-Wesley Publishing Co., 2000, pp. 517–526, https://doi.org/10.1145/344779.345074.

[14] J. Huang, Y. Tong, H. Wei, and H. Bao, *Boundary aligned smooth 3d cross-frame field*, in Proceedings of the 2011 SIGGRAPH Asia Conference, SA '11, ACM, 2011, pp. 1–8,

https://doi.org/10.1145/2024156.2024177.

[15] W. Jakob, M. Tarini, D. Panozzo, and O. Sorkine-Hornung, *Instant field-aligned meshes*, ACM Transactions on Graphics, 34 (2015), https://doi.org/10.1145/2816795.2818078.

[16] T. Jiang, X. Fang, J. Huang, H. Bao, Y. Tong, and M. Desbrun, *Frame field generation through metric customization*, ACM Trans. Graph., 34 (2015), art. 40, pp. 1–11, https://doi.org/10.1145/2766927.

[17] F. Kälberer, M. Nieser, and K. Polthier, *QuadCover - surface parameterization using branched coverings*, Computer Graphics Forum, 26 (2007), pp. 375–384, https://doi.org/10.1111/j.1467-8659.2007.01060.x.

[18] F. Knöppel, K. Crane, U. Pinkall, and P. Schröder, *Globally optimal direction fields*, ACM Trans. Graph., 32 (2013), art. 59, pp. 1–10, https://doi.org/10.1145/2461912.2462005.

[19] F. Knöppel, K. Crane, U. Pinkall, and P. Schröder, *Stripe patterns on surfaces*, ACM Trans. Graph., 34 (2015), art. 39, pp. 1–11, https://doi.org/10.1145/2767000.

[20] N. Kowalski, *Domain partitioning using frame fields : applications to quadrilateral and hexahedral meshing*, PhD thesis, Université Pierre et Marie Curie, 2013, http://www.sudoc.fr/179247484.

[21] N. Kowalski, F. Ledoux, and P. Frey, *A PDE based approach to multidomain partitioning and quadrilateral meshing*, in Proceedings of the 21st International Meshing Roundtable, X. Jiao and J.-C. Weill, eds., Springer Berlin Heidelberg, 2013, pp. 137–154, https://doi.org/10.1007/978-3-642-33573-0_9.

[22] W. c. Li, B. Vallet, N. Ray, and B. Lévy, *Representing higher-order singularities in vector fields on piecewise linear surfaces*, IEEE Transactions on Visualization and Computer Graphics, 12 (2006), pp. 1315–1322, https://doi.org/10.1109/TVCG.2006.173.

[23] E. H. Lieb and M. Loss, *Symmetry of the Ginzburg Landau minimizer in a disc*, Mathematical Research Letters, 1 (1994), pp. 701–715, https://doi.org/10.4310/MRL.1994.v1.n6.a7.

[24] J. H. Liu, *A First Course in the Qualitative Theory of Differential Equations*, Pearson Education, Inc, 2003.

[25] B. Merriman, J. Bence, and S. Osher, *Diffusion generated motion by mean curvature*, Tech. Report 92-18, University of California, Los Angeles, 1992, https://www.math.ucla.edu/applied/cam.

[26] B. Merriman, J. K. Bence, and S. J. Osher, *Diffusion generated motion by mean curvature*, in The Computational Crystal Grower's Workshop, AMS Selected Lectures in Mathematics, 1993, pp. 73–83.

[27] B. Merriman, J. K. Bence, and S. J. Osher, *Motion of multiple junctions: A level set approach*, Journal of Computational Physics, 112 (1994), pp. 334–363, https://doi.org/10.1006/jcph.1994.1105.

[28] S. A. Mitchell, *High fidelity interval assignment*, International Journal of Computational Geometry & Applications, 10 (2000), pp. 399–415, https://doi.org/10.1142/S0218195900000231.

[29] A. Myles, N. Pietroni, and D. Zorin, *Robust field-aligned global parametrization*, ACM Trans. Graph., 33 (2014), art. 135, pp. 1–14, https://doi.org/10.1145/2601097.2601154.

[30] M. Nieser, U. Reitebuch, and K. Polthier, *CubeCover parameterization of 3d volumes*, Computer Graphics Forum, 30 (2011), pp. 1397–1406, https://doi.org/10.1111/j.1467-8659.2011.02014.x.

[31] J. Palacios and E. Zhang, *Rotational symmetry field design on surfaces*, in ACM SIGGRAPH 2007 Papers, SIGGRAPH '07, ACM, 2007, https://doi.org/10.1145/1275808.1276446.

[32] D. Panozzo, E. Puppo, M. Tarini, and O. Sorkine-Hornung, *Frame fields: Anisotropic and non-orthogonal cross fields*, ACM Trans. Graph., 33 (2014), art. 134, pp. 1–11, https://doi.org/10.1145/2601097.2601179.

[33] N. Ray, W. C. Li, B. Lévy, A. Sheffer, and P. Alliez, *Periodic global parameterization*, ACM Trans. Graph., 25 (2006), pp. 1460–1485, https://doi.org/10.1145/1183287.1183297.

[34] N. Ray and D. Sokolov, *Robust polylines tracing for n-symmetry direction field on triangulated surfaces*, ACM Trans. Graph., 33 (2014), art. 30, pp. 1–11, https://doi.org/10.1145/2602145.

[35] N. Ray, D. Sokolov, and B. Lévy, *Practical 3d frame field generation*, ACM Trans. Graph., 35 (2016), art. 233, pp. 1–9, https://doi.org/10.1145/2980179.2982408.

[36] N. Ray, B. Vallet, L. Alonso, and B. Lévy, *Geometry-aware direction field processing*, ACM Trans. Graph., 29 (2009), art. 1, pp. 1–11, https://doi.org/10.1145/1640443.1640444.

[37] N. Ray, B. Vallet, W. C. Li, and B. Lévy, *N-symmetry direction field design*, ACM Trans. Graph., 27 (2008), art. 10, pp. 1–13, https://doi.org/10.1145/1356682.1356683.

[38] J. Rubinstein and P. Sternberg, *Homotopy classification of minimizers of the Ginzburg-Landau energy and the existence of permanent currents*, Communications in Mathe-

matical Physics, 179 (1996), pp. 257–263, https://doi.org/10.1007/BF02103722, https://link.springer.com/article/10.1007/BF02103722.

[39] S. J. Ruuth, B. Merriman, J. Xin, and S. J. Osher, *Diffusion-generated motion by mean curvature for filaments*, Journal of Nonlinear Science, 11 (2001), pp. 473–493, https://doi.org/10.1007/s00332-001-0404-x.

[40] Sandia National Laboratories, *The CUBIT geometry and mesh generation toolkit*, https://cubit.sandia.gov/.

[41] A. J. Schwartz, *A generalization of a Poincaré-Bendixson theorem to closed two-dimensional manifolds*, American Journal of Mathematics, 85 (1963), pp. 453–458, https://doi.org/10.2307/2373135.

[42] J. Solomon, A. Vaxman, and D. Bommes, *Boundary element octahedral fields in volumes*, ACM Trans. Graph., 36 (2017), art. 28, pp. 1–16, https://doi.org/10.1145/3065254.

[43] P. Sternberg and K.-S. Chen, *Dynamics of Ginzburg-Landau and Gross-Pitaevskii vortices on manifolds*, Discrete and Continuous Dynamical Systems, 34 (2013), pp. 1905–1931, https://doi.org/10.3934/dcds.2014.34.1905.

[44] M. Struwe, *On the asymptotic behavior of minimizers of the Ginzburg-Landau model in 2 dimensions*, Differential and Integral Equations, 7 (1994), pp. 1613–1624, https://doi.org/10.4310/mrl.1994.v1.n6.a7.

[45] K. Takayama, D. Panozzo, A. Sorkine-Hornung, and O. Sorkine-Hornung, *Robust and controllable quadrangulation of triangular and rectangular regions*, tech. report, ETH Zurich, 2013, https://igl.ethz.ch/projects/sketch-retopo/.

[46] K. Takayama, D. Panozzo, and O. Sorkine-Hornung, *Pattern-based quadrangulation for n-sided patches*, Comput. Graph. Forum, 33 (2014), pp. 177–184, https://doi.org/10.1111/cgf.12443.

[47] A. Vaxman, M. Campen, O. Diamanti, D. Panozzo, D. Bommes, K. Hildebrandt, and M. Ben-Chen, *Directional field synthesis, design, and processing*, in Computer Graphics Forum, vol. 35, Wiley Online Library, 2016, pp. 545–572, https://doi.org/10.1145/2988458.2988478.

[48] R. Viertel, M. Staten, and F. Ledoux, *Analysis of non-meshable automatically generated frame fields*, in Proceedings of the 25th International Meshing Roundtable, 2016, http://imr.sandia.gov/papers/abstracts/Vi831.html.

[49] R. Wang, S. Gao, Z. Zheng, and J. Chen, *Frame field guided topological improvement for hex mesh using sheet operations*, Procedia Engineering, 163 (2016), pp. 276–288, https://doi.org/10.1016/j.proeng.2016.11.060.